JOURNAL OF GEOPHYSICAL RESEARCH, VOL. 115, D00H15, doi:10.1029/2009JD012130, 2010

Click Here for Full Article

Using airborne high spectral resolution lidar data to evaluate combined active plus passive retrievals of aerosol extinction profiles

S. P. Burton,[1] R. A. Ferrare,[2] C. A. Hostetler,[2] J. W. Hair,[2] C. Kittaka,[1,3] M. A. Vaughan,[2] M. D. Obland,[2] R. R. Rogers,[2] A. L. Cook,[2] D. B. Harper,[2] and L. A. Remer[4]

Received 31 March 2009; revised 25 September 2009; accepted 5 October 2009; published 3 March 2010.

[1] We derive aerosol extinction profiles from airborne and space-based lidar backscatter signals by constraining the retrieval with column aerosol optical thickness (AOT), with no need to rely on assumptions about aerosol type or lidar ratio. The backscatter data were acquired by the NASA Langley Research Center airborne High Spectral Resolution Lidar (HSRL) and by the Cloud-Aerosol Lidar with Orthogonal Polarization (CALIOP) instrument on the Cloud-Aerosol Lidar and Infrared Pathfinder Satellite Observation (CALIPSO) satellite. The HSRL also simultaneously measures aerosol extinction coefficients independently using the high spectral resolution lidar technique, thereby providing an ideal data set for evaluating the retrieval. We retrieve aerosol extinction profiles from both HSRL and CALIOP attenuated backscatter data constrained with HSRL, Moderate-Resolution Imaging Spectroradiometer (MODIS), and Multiangle Imaging Spectroradiometer column AOT. The resulting profiles are compared with the aerosol extinction measured by HSRL. Retrievals are limited to cases where the column aerosol thickness is greater than 0.2 over land and 0.15 over water. In the case of large AOT, the results using the Aqua MODIS constraint over water are poorer than Aqua MODIS over land or Terra MODIS. The poorer results relate to an apparent bias in Aqua MODIS AOT over water observed in August 2007. This apparent bias is still under investigation. Finally, aerosol extinction coefficients are derived from CALIPSO backscatter data using AOT from Aqua MODIS for 28 profiles over land and 9 over water. They agree with coincident measurements by the airborne HSRL to within ±0.016 km^{-1} ± 20% for at least two-thirds of land points and within ±0.028 km^{-1} ± 20% for at least two-thirds of ocean points.

Citation: Burton, S. P., et al. (2010), Using airborne high spectral resolution lidar data to evaluate combined active plus passive retrievals of aerosol extinction profiles, *J. Geophys. Res.*, *115*, D00H15, doi:10.1029/2009JD012130.

1. Introduction

[2] Accurate aerosol measurements are needed in the study of climate, since aerosols affect climate by scattering and absorbing solar radiation and also by altering the lifetime and development of clouds. Aerosols are the source of the biggest uncertainties in climate forcing in climate models [*Hansen et al.*, 2007]. Aerosol radiative forcing depends strongly on the vertical distribution of aerosols [*Haywood et al.*, 1997]. For example, scattering particles exhibit a greater forcing when most of the aerosol mass is located in the lower troposphere because of the increase in aerosol size with relative humidity. Absorbing aerosols, in contrast, produce a greater radiative forcing when the aerosol mass is above cloudy layers or when the underlying surface albedo is high [*Haywood et al.*, 1997]. Accurate measurements of the vertical distribution of aerosols are therefore an important requirement for understanding climate change.

[3] Lidar remote sensing is a valuable means of measuring the vertical distribution of aerosol properties. Elastic backscatter lidar instruments are commonly used [e.g., *Bosenberg et al.*, 2001] to derive aerosol backscatter and extinction coefficients. An elastic backscatter lidar such as that on board the Cloud-Aerosol Lidar and Infrared Pathfinder Satellite Observation (CALIPSO) satellite directly measures the attenuated backscatter signal, which is the product of the backscatter coefficient and the two-way transmission between the lidar and the backscattering volume in question. Both the particulate backscatter coefficient and particulate extinction coefficient at a given range are unknown variables to be retrieved with a single equation relating them, so the retrieval is underdetermined. The two unknowns can be related to each other by the aerosol extinction-to-backscatter ratio or "lidar ratio," S_a. The lidar ratio (or its inverse) is frequently either assumed or inferred from additional measurements and used as a means of

[1]Science Systems and Applications Inc., Hampton, Virginia, USA.
[2]NASA Langley Research Center, Hampton, Virginia, USA.
[3]Deceased 18 March 2009.
[4]NASA Goddard Space Flight Center, Greenbelt, Maryland, USA.

Copyright 2010 by the American Geophysical Union.
0148-0227/10/2009JD012130$09.00

solving the lidar equation [*Fernald et al.*, 1972; *Klett*, 1981; *Fernald*, 1984]. The operational CALIPSO algorithm must infer a value of S_a for each aerosol layer in order to retrieve aerosol backscatter and extinction coefficients from measurements of attenuated backscatter. The goal of the operational CALIPSO algorithm is to define S_a to within 30% [*Omar et al.*, 2009], a goal which can often be reached with incomplete knowledge of the aerosol type. However, error in the assumed value of S_a creates errors in both the backscatter and extinction profiles [*Sasano et al.*, 1985; *Fernald*, 1984]. In CALIPSO processing, furthermore, errors due to incorrect lidar ratios propagate downward as the attenuation by upper layers is corrected in the retrieval of lower layers [*Young and Vaughan*, 2009; *Winker et al.*, 2009], so errors are of particular concern for near-surface applications, like air quality studies. The actual value of the aerosol lidar ratio depends on particle composition, size distribution, and morphology. It can vary widely ($10 < S_a < 110$) [e.g., *Ferrare et al.*, 2001] and unfortunately is not well known. Since uncertainties in the lidar ratio are a potential major source of uncertainty in the CALIPSO aerosol backscatter and extinction retrievals, it is worthwhile to examine any opportunity to improve lidar ratio estimates. In fact, the CALIPSO extinction algorithm refines the estimation of the lidar ratio in certain cases: in the presence of elevated layers, the layer optical depth can be determined by the reduction in the clear air signal above and below the layer [*Young and Vaughan*, 2009]. In these cases, adjustments are made to S_a within the layer to produce a match with the observed layer optical depth. However, opportunities to refine S_a this way are rare. The active-passive retrieval described in this work is a similar method, but uses an observed column optical depth from another instrument to constrain the retrieval over the entire column.

[4] The desire to avoid assuming a value for S_a has led to various studies to retrieve profiles of both aerosol extinction and backscatter coefficients from lidar data by constraining the solution with column aerosol information from coincident satellite measurements. A successful implementation of such a technique would potentially improve aerosol extinction retrievals from CALIPSO. *Kaufman et al.* [2003] invert lidar data from the airborne LEANDRE 1 lidar using a set of aerosol models having one fine plus one coarse mode and predefined refractive indices. Spectral reflectance values are calculated from the lidar profiles for each of the 20 combinations of fine and coarse modes and then the measured spectral reflectance from the Moderate-Resolution Imaging Spectroradiometer (MODIS) is used to choose among the models. *Leon et al.* [2003] describe a method that is similar in many ways, but their retrieval is constrained by the MODIS optical thickness interpolated to the lidar wavelengths of 532 nm and 1064 nm and by the MODIS effective radius, rather than the reflectance. These techniques produce more aerosol information than methods that retrieve only aerosol backscatter and extinction coefficients, but with some disadvantages. For example, *Leon et al.* [2003] point out that the relevance of the aerosol models is key to the retrievals; the models cannot completely capture the effects of nonsphericity of dust particles, and they neglect the possibility of two coarse modes, such as dust and sea salt. R. Fernandez-Borda et al. (unpublished manuscript, 2009) partially address these issues by making use of depolarization data to resolve dust and sea salt in the coarse mode for a similar retrieval. These techniques require a dark background for MODIS observations, and are only useful over glint-free ocean, although it may be expected that polarization sensitive retrievals from the Aerosol Polarimetry Sensor (APS) on the Glory mission can ultimately overcome this issue due to the depolarizing effect of the surface. Another active-passive retrieval technique that uses aerosol models, the Constrained Ratio Aerosol Model-Fit (CRAM) technique, described by *McPherson et al.* [2010], constrains the retrievals by requiring that the spectral ratios of retrieved aerosol properties fall within ranges for aerosol models determined from the Aerosol Robotic Network (AERONET) [*Holben et al.*, 1998]. Since the CRAM technique does not require simultaneous passive measurements, it has the potential to make fuller use of lidar measurements even at night. The use of the 1064 nm channels in these retrievals has advantages and disadvantages. Unquestionably these retrievals provide more information than single channel retrievals. However, the 1064 nm attenuated backscatter observations commonly have relatively smaller signal-to-noise ratios, and currently have greater calibration uncertainty, 10% (M. A. Vaughan et al., On the spectral dependence of backscatter from cirrus clouds: Assessing CALIOP's 1064 nm calibration assumptions using Cloud Physics Lidar measurements, submitted to *Journal of Geophysical Research*, 2009) compared to 5% in the 532 nm channel [*Powell et al.*, 2009]. While this is not to be seen as an impediment to obtaining useful retrievals, these greater uncertainties are presently a factor in simultaneous two-channel retrievals but not in simpler retrievals that treat the 532 nm measurements independently of the 1064 nm channel. A single-channel retrieval may be successful in some cases where the two-channel retrievals struggle. The more important limitation of each of these retrievals, as well as the operational CALIPSO retrieval, is the necessity of obtaining accurate aerosol optical models. Techniques that do not rely on models have an advantage in the presence of aerosols that may not be well characterized by the models, for example mixes of multiple types.

[5] *McGill et al.* [2003] retrieve aerosol from airborne Cloud Physics Lidar (CPL) measurements using a variety of strategies, some free from any assumptions of particular aerosol models. In the presence of an elevated aerosol layer or thin cloud layers with measurable clear-air signals beneath, they are able to retrieve aerosol extinction profiles from lidar data alone using the transmission loss through the layer, similar to *Young* [1995]. In other cases, they use the aerosol optical thickness (AOT) from ground-based or airborne Sun photometers [see also *Fernald et al.*, 1972]. *Stephens et al.* [2001] proposed a method to invert lidar profiles from space using the total column optical depth as a constraint by an optimal estimation method and illustrated its use on three profiles from the Lidar in Space Technology Experiment (LITE) that flew aboard the space shuttle in September 1994. Methods that use the column aerosol optical thickness to constrain the retrieval, including the experiment described in this report, assume that the lidar extinction-to-backscatter ratio is constant throughout the altitude range. One recent study using this technique with satellite AOT as a constraint is described by *Ferrare et al.*

[2006]. They derive aerosol extinction profiles from the NASA Langley UV-DIAL lidar. A time series of satellite-observed column AOT values along the airborne lidar flight track is formed. For each point along the track, the retrieval of aerosol extinction from backscatter returns is constrained by requiring that the resulting AOT matches the satellite AOT.

[6] The same technique as used by *Ferrare et al.* [2006] is used here. In this case, the retrieval is constrained using aerosol optical thickness measured from a satellite instrument such as MODIS or the Multiangle Imaging Spectroradiometer (MISR). This is a simple, straightforward technique that does not rely on aerosol models and can be done over land or ocean. Aerosol extinction is retrieved from total (i.e., aerosol plus molecular) attenuated backscatter profiles at 532 nm obtained by the airborne NASA Langley High Spectral Resolution Lidar (HSRL) [*Hair et al.*, 2008] and from CALIPSO. The combined active and passive retrieval described here is designed especially for a backscatter lidar like the Cloud-Aerosol Lidar with Orthogonal Polarization (CALIOP) on CALIPSO, but applying it to the attenuated backscatter signal data from the HSRL provides a unique opportunity, a "truth" measurement to use in validating and characterizing the constrained backscatter retrieval. This is because the HSRL technique yields an independent derivation of aerosol extinction coefficient at 532 nm. The NASA Langley airborne HSRL extinction measurements were validated recently by *Rogers et al.* [2009]. The HSRL and CALIPSO instruments are described in section 2. The retrieval technique is described in more detail in section 3. A prerequisite for the retrieval is an accurate coincident measurement of aerosol optical thickness, so we accordingly begin by using the Langley HSRL measurements of aerosol optical thickness to evaluate AOT from the MODIS and MISR satellite instruments (section 4). Next, we use the HSRL measurements again to validate the procedure and assumptions of the active-passive retrieval. We approach the testing in section 5 and section 6 by applying the retrieval to attenuated backscatter signals obtained by HSRL, producing retrieved aerosol extinction coefficients that can be unambiguously compared with the extinction coefficient measured by the same instrument using the HSRL technique. Finally, in section 7 we apply the active-passive retrieval to attenuated backscatter data obtained by the CALIOP instrument on CALIPSO, and assess the resulting aerosol extinction coefficients by comparison again with coincident HSRL extinction measurements.

2. Instrument Descriptions

[7] The CALIPSO satellite was launched 28 April 2006 in formation with the Aqua and CloudSat satellites. Initial observations occurred on 7 June 2006. The primary instrument on board is the CALIOP sensor, the first satellite lidar optimized for cloud and aerosol observations [*Winker et al.*, 2007]. It provides measurements of backscattered signal at two wavelengths, 1064 nm and 532 nm, and depolarization at 532 nm. The vertical resolution of the level 1 total attenuated backscattering data is 30 m below 8.2 km, and data are provided approximately every 0.05 s or 1/3 km horizontally. Above 8.2 km, both the horizontal and vertical resolution are less [*Hunt et al.*, 2009]. The horizontal averaging for the CALIPSO aerosol products is described by *Young and Vaughan* [2009]. The products are reported on a nominal 40 km grid; the vertical resolution is 120 m between the surface and 20.2 km and 360 m above that altitude [*Anselmo et al.*, 2007].

[8] As of the writing of this report, the operational retrieval of aerosol extinction coefficient from CALIOP backscatter signals has not yet been fully validated and has been released only in provisional form. The operational algorithms for the aerosol classification and retrieval are described by *Liu et al.* [2009], *Omar et al.* [2009], and *Young and Vaughan* [2009]. In these algorithms, aerosol layers are identified as described by *Vaughan et al.* [2009] and assigned to one of six aerosol types (desert dust, biomass burning, clean continental, polluted continental, marine, and polluted dust) each having a characteristic lidar ratio [*Omar et al.*, 2009]. Aerosol models for the categories, including lidar ratios, were derived from field measurements and AERONET data [*Holben et al.*, 1998] and the CALIOP retrieval categorizes observed layers among the six types using a decision tree. The goal of this part of the CALIOP algorithm is to determine S_a to an uncertainty of no more than 30% [*Omar et al.*, 2009].

[9] The airborne HSRL instrument also measures backscattered signal at 532 nm and 1064 nm, and measures depolarization at both wavelengths [*Hair et al.*, 2008]. The vertical resolution of these measurements is 30 m, and the horizontal averaging is 10 s (about 1 km) [*Rogers et al.*, 2009]. In addition, the aerosol extinction coefficient at 532 nm is derived directly with the HSRL technique [*Grund and Eloranta*, 1991]. This is accomplished by taking advantage of the difference in spectra between the Cabannes (molecular) and Mie (aerosol) scattering [*She*, 2001] to infer the molecular component of the attenuated backscatter signal. The observed molecular backscattering is attenuated by extinction. Therefore the attenuated molecular signal can be compared to the molecular backscattering coefficient from a known atmospheric density profile to derive the attenuation due to extinction by both aerosol and molecules. Since the molecular extinction coefficient is also known from the density profile, the aerosol extinction coefficient is thus derived. For more details of the measurement technique, see the work by *Hair et al.* [2008]. The HSRL aerosol extinction profiles have a vertical resolution of 300 m, and the horizontal averaging is 60 s (~6 km) [*Rogers et al.*, 2009]. They extend from ~300 m above the surface to ~2500 m below the aircraft. The 300 m limit at the low end of the profile is to avoid extending the retrieval to the surface and below. The 2500 m near-range limit is to insure full overlap between the outgoing laser and the receiver field of view. In the comparisons in the remainder of this paper, the extinction derived using the HSRL technique will be referred to as the *measured* aerosol extinction coefficient, while the results of the active-passive retrieval introduced in this paper will be called *calculated* or *retrieved.*

[10] The HSRL instrument has flown aboard the NASA Langley King Air B200 on more than 190 flights since March 2006 during a variety of missions. Table 1 lists all the missions on which the airborne HSRL has been deployed up to July 2008. Of these flights, 68 include segments coordinated with CALIPSO overpasses, providing

Table 1. Missions Flown by the NASA Langley B200 King Air With the High Spectral Resolution Lidar On Board[a]

Mission	Dates	Location	Number of B200 Flights	Number of CALIPSO Underflights
MILAGRO	1–31 Mar 2006	Mexico City area	20	0
CC-VEX	14 Jun to 17 Aug 2006	Mid-Atlantic United States	15	11
GoMACCS	27 Aug to 28 Sep 2006	Texas/Gulf of Mexico	27	10
San Joaquin	8–20 Feb 2007	San Joaquin Valley, California	15	0
CHAPS	3–29 Jun 2007	Oklahoma and Kansas	22	8
CATZ	12 Jul to 11 Aug 2007	Mid-Atlantic United States	12	4
Caribbean	16 Jan to 3 Feb 2008	Caribbean Sea	20	7
ARCTAS1	30 Mar to 22 Apr 2008	Alaska, Arctic Circle	27	12
ARCTAS2	16 Jun to 13 Jul 2008	Northwest Territories and Alberta, Canada	22	11
Other[b]	24 May 2006 to 20 Mar 2008	Mid-Atlantic United States	11	5

[a]Abbreviations are as follows: ARCTAS, Arctic Research of the Composition of the Troposphere from Aircraft and Satellites; CATZ, CALIPSO and Twilight Zone; CC-VEX, CALIPSO-CloudSat Validation Experiment; CHAPS, Cumulus Humilis Aerosol Processing Study; GoMACCS, TexAQS/GoMACCS, Texas Air Quality Study/Gulf of Mexico Atmospheric Composition and Climate Study; MILAGRO, Megacity Initiative: Local and Global Research Observations.

[b]HSRL flights not part of other missions, local to NASA Langley Research Center.

an opportunity to validate extinction retrievals from the CALIOP sensor. Several of these campaigns have also provided opportunities to evaluate the aerosol extinction profiles measured by the HSRL. *Rogers et al.* [2009] perform comparisons of HSRL extinction profiles from the MILAGRO campaign with profiles derived from airborne Sun photometer and in situ measurements and found that the HSRL profiles were within the typical state-of-the-art systematic error of 15–20% at visible wavelengths [*Schmid et al.*, 2006].

3. Aerosol Extinction Retrieval

[11] To retrieve aerosol extinction coefficient from the attenuated backscatter signal, we implement a Fernald near-field solution [*Fernald*, 1984] that solves step-by-step from near the aircraft toward the ground or ocean surface. The aerosol extinction to backscatter ratio, or lidar ratio, S_a, is assumed to be known and constant with range. However, for this retrieval, rather than assume a value for S_a by inferring an aerosol type, the lidar ratio is determined by requiring that the column integral of the aerosol extinction coefficient corresponds to a column AOT value obtained from a coincident MODIS or MISR measurement. The solution is obtained in a straightforward way by forming the Fernald equation and the numerical integration into root-finding form (i.e., an equation with one side equal to zero) and solving for S_a with an off-the-shelf nonlinear root finder that uses Muller's method [*Muller*, 1956; see also *Press et al.*, 1992]. Measurement noise can sometimes cause unwanted roots (for example, negative ones); these are avoided by limiting the solution to the regime where the equation is well behaved, determined empirically by solving the equation for a coarsely gridded vector of potential S_a values. The upper limit for the solution in practice is generally between 100 and 200 sr, and the lower limit is taken to be zero. There is no need to invert the equation for S_a analytically. By these means, the ratio of aerosol extinction to backscattering is free to vary with time and location along the flight track, although the method still depends on the underlying assumption that S_a is constant with altitude.

[12] The choice of range value (i.e., altitude) to use for initializing the Fernald solution can affect the success of the retrieval. Specifically, in the case of CALIPSO backscatter data, starting the retrieval where the signal-to-noise ratio is small causes instability in the retrieval. To address this problem in the CALIPSO active plus passive retrieval, the vertical feature mask (VFM) product is used. The VFM is a set of discrete tags mapped onto the full resolution CALIPSO measurement space. Each element is coded according to the result of the scene classification algorithm as either clear, cloud, aerosol, surface, subsurface, stratospheric, or totally attenuated. For the purpose of this retrieval, the starting altitude is set 2000 m above the highest air mass noted in the VFM as anything other than clear air, regardless of whether it is identified as aerosol or something else. Above this altitude, attenuation in the backscatter signal is taken to be due only to molecular and ozone scattering. The conservative buffer of 2000 m of nominally clear air is included in the retrieval to account for any imprecision or uncertainty in the location of the highest feature top.

[13] In the case of HSRL backscatter retrievals, the signal-to-noise ratio is much higher and including noise in a clear air region at the start of a profile does not make the Fernald solution unstable. However, for consistency with the CALIPSO retrieval and to avoid possible bias in clear air regions with small signal-to-noise ratio, the starting range of the retrieval is taken at the lower boundary of any clear air region below the aircraft, where the region of clear air is defined empirically by examining the measured extinction coefficient profile. The attenuated backscatter signal is calibrated at 1500 m below the aircraft, so this retrieval includes a correction for molecular attenuation between the calibration point and the point where the retrieval begins.

4. Aerosol Optical Thickness

[14] There are several satellite measurements of AOT that can potentially be used to constrain the extinction retrieval from either CALIPSO or HSRL backscatter data. This analysis focuses primarily on the Aqua MODIS AOT measurements since this sensor provides the best coincidence with the CALIPSO measurements. The MODIS and MISR instruments on the Terra satellite are additional options, although with fewer coincidences. Also, the AOT

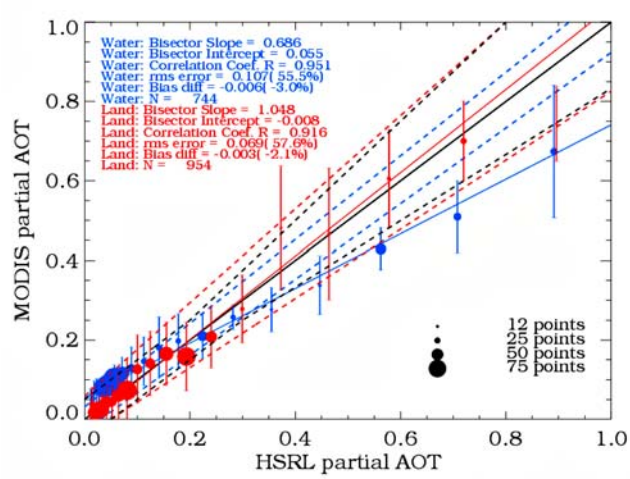

Figure 1. Aerosol optical thickness from the Moderate-Resolution Imaging Spectroradiometer (MODIS) on Aqua, compared to aerosol optical thickness (AOT) measured by the airborne High Spectral Resolution Lidar (HSRL) instrument. Adjustments have been made to convert from the MODIS wavelength and to estimate the fraction of MODIS AOT in the altitude range over which the HSRL AOT measurements are made. Additional binning and averaging beyond what is described in the text was performed for plotting clarity, to avoid a dense scatter of indistinguishable points. The red and blue dots represent binned averages over land and water, respectively, with the size of the dot proportional to the number of observations per bin. The bin sizes are constant in logarithm space, chosen because of the relative abundance of points with small AOT. The bars designate the standard deviation within each bin. This binning does not apply to the linear bisector regressions, which are illustrated as solid lines in red for land and blue for water. Dashed lines are ±0.03 ± 0.05 AOT (for ocean in blue) and ±0.05 ± 0.15 AOT (for land in red). These are the estimated standard deviations as given by *Remer et al.* [2005]. The black dashed lines represent the larger of 0.05 or 20% of AOT.

derived directly from HSRL using the HSRL technique was used for testing the retrievals, as discussed below. In order to use satellite derived (MODIS or MISR) aerosol optical thickness data with the 532 nm attenuated backscatter signal from HSRL or CALIPSO, some adjustments are necessary. The MODIS aerosol optical thickness is reported at a wavelength of 550 nm, and MISR at 558 nm. Because the wavelength difference is small, the assumption of an inverse wavelength relationship for extinction is sufficient to convert the AOT to the lidar wavelength. In addition, since the HSRL aerosol measurements are made from aircraft and do not include the stratospheric portion of the aerosol optical depth, an assumed constant value of 0.004 is subtracted from the satellite value. This is the recent background stratospheric optical depth for northern midlatitudes estimated for the lidar wavelength from solar occultation satellite data [*Thomason and Peter*, 2006; *Thomason et al.*, 2008] and from long-term midlatitude ground based lidar observations of stratospheric aerosol [*Jäger*, 2005, Figure 3] The HSRL operational AOT estimate actually refers to a greater portion of the atmosphere than the extinction profile does, since the extinction profile does not go below approximately 300 m above the ground and the AOT estimate includes a correction to extend the range [*Rogers et al.*, 2009]. For the sake of comparison, the active-passive retrieval is performed only for levels where the measured aerosol extinction coefficient is defined. Therefore, the AOT from both HSRL and the satellites are reduced by an additional factor, defined as the fraction of HSRL AOT present in the retrieved levels. This partial column optical depth is used to constrain the retrievals.

[15] The retrieval is done only on cloud-free profiles. When performing the retrieval on CALIPSO attenuated backscatter data, we screen for clouds using the 1 km cloud layer product, which gives profile by profile information on the location of cloud layers for signals that were strong enough to detect at 1 km resolution [*Vaughan et al.*, 2004]. Data below clouds are removed before the profiles are averaged to a coarser horizontal resolution of 80 km for the retrieval. If no data remain down to at least 300 m above the surface for the averaged profile, then that profile is not retrieved. The HSRL backscatter retrieval is done profile by profile without further horizontal averaging. HSRL observations are cloud cleared by performing a convolution of the measured signal at 532 nm with a Haar wavelet to enhance edges [e.g., *Davis et al.*, 2000], combined with an algorithm to set a flight-by-flight threshold that separates the generally sharper cloud edges from the less pronounced aerosol feature boundaries in each lidar profile.

[16] A comparison of the aerosol optical thickness observations from MODIS on Aqua and from HSRL, adjusted as discussed above, is illustrated in Figure 1. For the retrieval, the adjustments are done on a profile-by-profile basis. However, for one-to-one correspondence in the AOT comparisons, AOT values for every HSRL profile that falls beneath a given MODIS pixel and within 3 hours of the MODIS observation are averaged together. In general, the averaging can be from 1 to ~20 profiles, depending on how the flight path intersects the observation pixel. This averaging is done to preserve statistical independence between points in the comparison. However, if the HSRL flies within the MODIS pixel two or more discrete times during a flight, the MODIS pixel will be represented multiple times in the comparisons, in order to avoid averaging HSRL measurements at distinct observation times.

[17] The MODIS data used here are from Collection 5. Prelaunch estimates of uncertainties are shown, as provided by *Remer et al.* [2005] and subsequently validated for Collection 5 AOT by *Remer et al.* [2008]. We follow the recommendation to use the quality assurance (QA) flags to filter the data, requiring QA = 3 over land and QA > 0 over water [*Remer et al.*, 2008]. Coincidences for HSRL flights up to July 2008 are included. Compared to the HSRL measurement, MODIS Aqua AOT over water are biased high for lower values of AOT (less than about 0.2) and low for high values. Errors at low values of AOT are not unexpected, due to the difficulty of the measurements. However, the low bias at higher values is particularly striking. For the small set of coincidences over water with AOT greater than 0.4, 95% of the observations are outside the reported uncertainty. The number of observations rep-

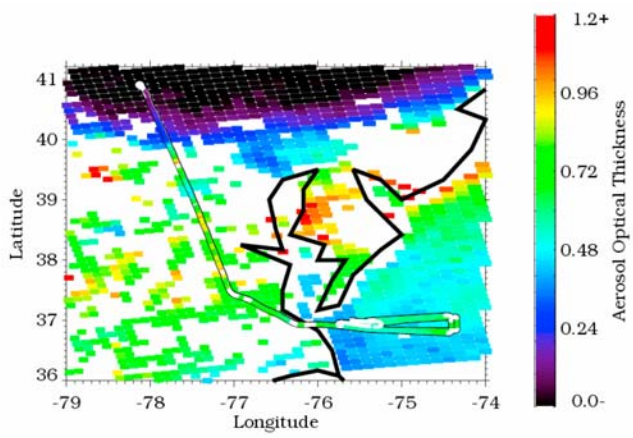

Figure 2. Map showing the AOT from MODIS Aqua at 550 nm over the eastern United States and Atlantic Ocean off the coast of Virginia on 4 August 2007. The MODIS data granule is from 1825 UT. The data have been filtered using the QA flags according to *Remer et al.* [2008]. The B200 flight track is also shown, color coded by AOT as measured by the HSRL instrument at 532 nm, between 1636 UT and 1954 UT. For this figure, no wavelength shift has been applied to account for the small difference in wavelength between the two instruments.

resented in the large-AOT regime is small, however, and the bulk of these comparisons, 85%, occur during just three flights in August 2007. The apparent observed bias over water contrasts with measurements over land, in which no clear bias between MODIS and HSRL is evident, even on the same flights. Figure 2 shows an example from 4 August 2007 in the form of a map of MODIS Aqua aerosol optical thickness with the HSRL measurement overlaid on the B200 flight track. The flight took place over the eastern United States and over the Atlantic Ocean off the coast of Virginia, between 1636 UT and 1954 UT, and the Aqua observation occurred at 1825 UT. Over land, excellent agreement is evident, but over water there is a discrepancy of approximately 30%. The partial column AOT for the ocean segment is shown as a time series in Figure 3. In this figure, both MODIS on Aqua and MODIS on Terra are shown, with adjustments as described above to convert the MODIS AOT to the HSRL wavelength of 532 nm and so that all values refer to the same partial column. The Terra overpasses that include the HSRL flight track occurred a few hours earlier, at 1505 and 1645 UT. Even given the time difference the difference between Aqua MODIS and Terra MODIS is surprising. Despite poorer time coincidence, there is no overall bias between the Terra MODIS AOT and the HSRL AOT. Also shown in the figure is AOT from the Polarization and Anisotropy of Reflectances for Atmospheric Sciences Coupled With Observations From a Lidar (PARASOL) instrument. PARASOL is a wide-field imaging radiometer and polarimeter and another member of the "A-train" satellite constellation, trailing Aqua by about 3 min. Observations at the PARASOL wavelength of 670 nm are converted to the smaller wavelength using an Angstrom coefficient derived from the PARASOL data at 670 nm and 865 nm. This is a rough calculation, but the PARASOL data appear to also agree better with MODIS on Terra and HSRL than MODIS on Aqua. The reason for the bias is unknown. The large-scale validation work presented by *Remer et al.* [2008] does not find a bias; however, differences between Aqua and Terra ocean retrievals, within the error bars, are visible in Figure 1 of that work. It may be possible that a nonrandom subset of observations over water may be biased. Figure 4 illustrates a much larger set of comparisons with aerosol optical thickness observed by PARASOL. Over 3 million observations over water were compared globally for a period of about 9 months. In this larger data set, a bias between the two instruments for large values of AOT is evident at least at large scattering angles. The figure illustrates scattering angles between 160° and 180°. Further investigation into the character and circumstances of the bias is needed.

[18] Figure 5 shows a comparison between HSRL and MODIS on Terra. Again MODIS overestimates with respect to HSRL for small AOT. However, in this case, 47% of the observations over water with AOT greater than 0.4 are within the reported uncertainty; there is no clear bias at very large AOT as in the Aqua case.

[19] Finally, we compare MISR aerosol optical thickness to AOT derived from the HSRL measurements. The comparison is shown in Figure 6. There are fewer coincidences between MISR and HSRL and essentially none at large AOT. The error envelope shown in the figure is the error estimate given by *Kahn et al.* [2005] that includes approximately two-thirds of all comparisons between MISR and coincident AERONET observations, that is, 0.05 or 20% of AOT, whichever is larger. In comparison with HSRL, 63% of comparisons over water and 68% over land fall within the given envelope. Each of these figures also includes the

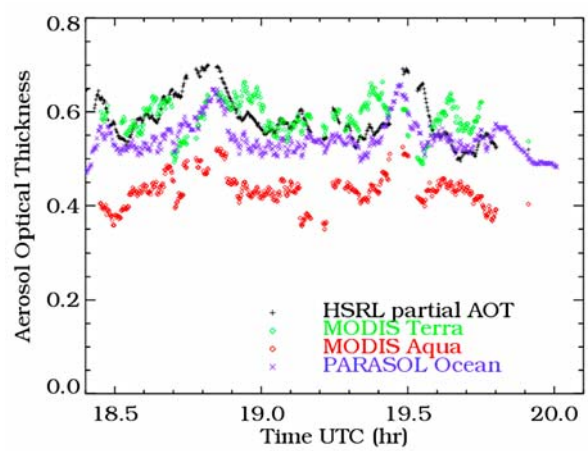

Figure 3. A time series of aerosol optical thickness at 532 nm for the portion of the HSRL flight over water on 4 August 2007. All AOT values are partial column values that refer to the portion of the atmospheric column observed in HSRL extinction measurements (as described in the text). Wavelength conversions are described in the text. Black shows partial column AOT from HSRL, green shows MODIS on Terra, red shows MODIS on Aqua, and purple shows Polarization and Anisotropy of Reflectances for Atmospheric Sciences Coupled With Observations From a Lidar (PARASOL).

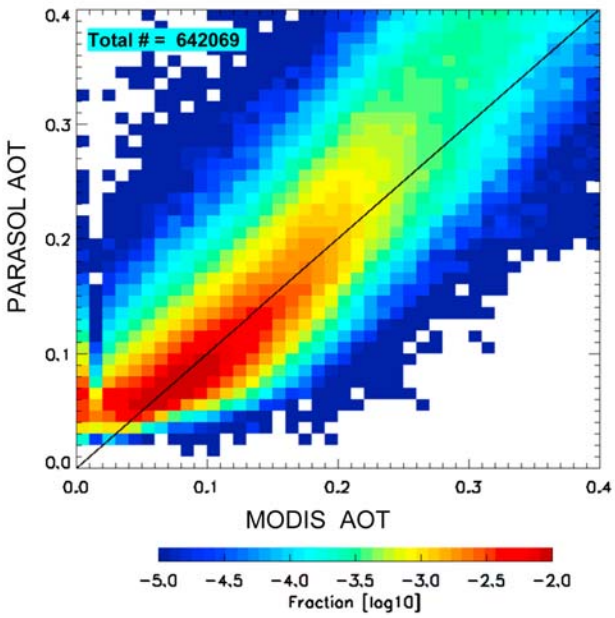

Figure 4. Probability density function (pdf) illustrating global comparisons between MODIS Aqua AOT over ocean and PARASOL at 550 nm for a subset of cloud-free MODIS observations with scattering angles between 160° and 180°, between 15 June 2006 and 7 March 2007. Measurements from the two instruments tend to diverge at large values of AOT.

linear bisector regression line, which was chosen rather than the ordinary least squares regression since both axes represent measurements [*Isobe et al.*, 1990].

[20] The criterion for coincidence in time is 3 hours, as mentioned above. This criterion is applied both for the AOT comparisons discussed here and for the retrievals that follow. Limiting the criterion further, to 30 min, does not affect the comparisons very much, improving the linear correlation coefficient from 0.753 to 0.792 for the case of the MISR constraint over land, from 0.916 to 0.937 for the

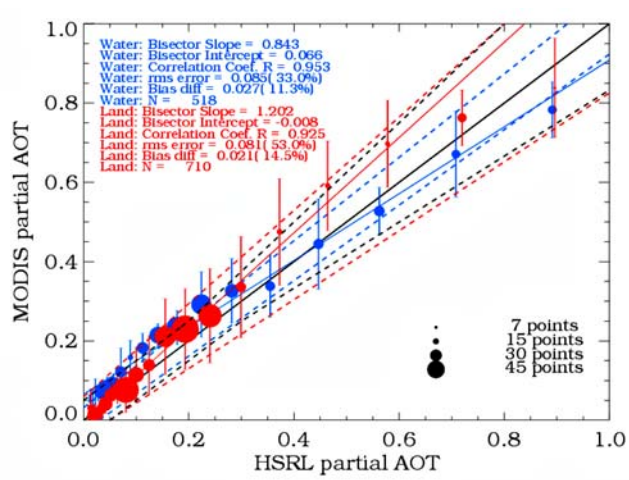

Figure 5. Same as Figure 1 but for MODIS on Terra.

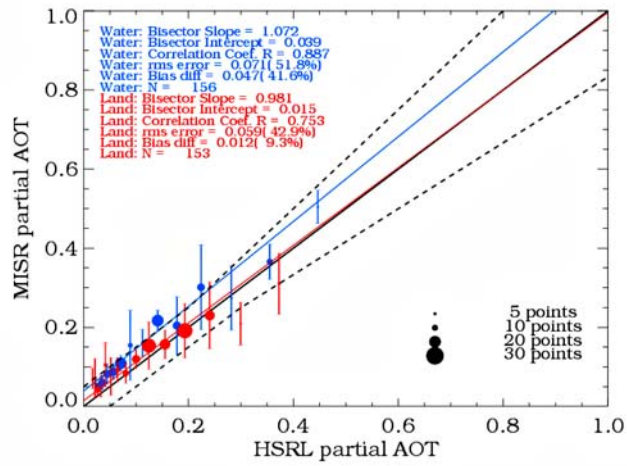

Figure 6. Same as Figure 1 but for Multiangle Imaging Spectroradiometer (MISR) instead of MODIS. The dashed lines represent uncertainty as the larger of 0.05 or 20% of AOT, which is given by *Kahn et al.* [2005] as the uncertainty envelope in which approximately two-thirds of the MISR aerosol optical thickness falls, in comparison with the Aerosol Robotic Network (AERONET).

Aqua MODIS constraint over land, and smaller improvements (or decreases) in the other cases.

[21] The published uncertainties in AOT from MODIS and MISR are shown again in Figure 7, along with the estimated error in AOT from the operational CALIPSO retrievals due to assumed 10% and 30% errors in the lidar ratio [*Winker et al.*, 2009]. The uncertainty in the CALIPSO AOT values increases with increasing aerosol optical thickness, while the uncertainties in the MODIS and MISR AOT values decrease. Therefore, to the right of the crossing point,

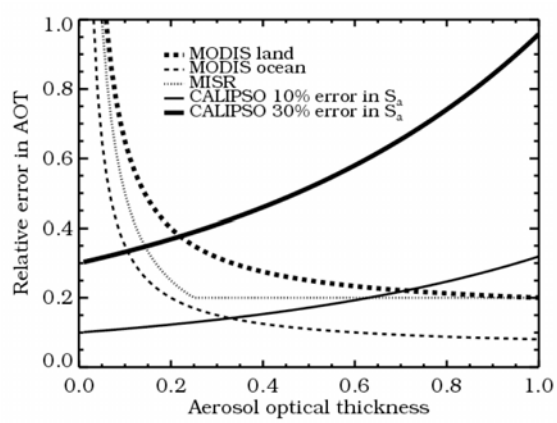

Figure 7. Relative error in AOT associated with the uncertainty with MODIS (bold dashed line for water and dashed line for land) and MISR (dotted line) and with assumed 10% (solid line) and 30% (bold solid line) uncertainty in CALIPSO S_a [*Winker et al.*, 2009]. The MODIS and MISR estimates are taken from the work of *Remer et al.* [2005] and *Kahn et al.* [2005], respectively. The relative error in AOT for CALIPSO increases with increasing AOT, while the relative errors in the MISR and MODIS AOT measurements decrease with increasing AOT.

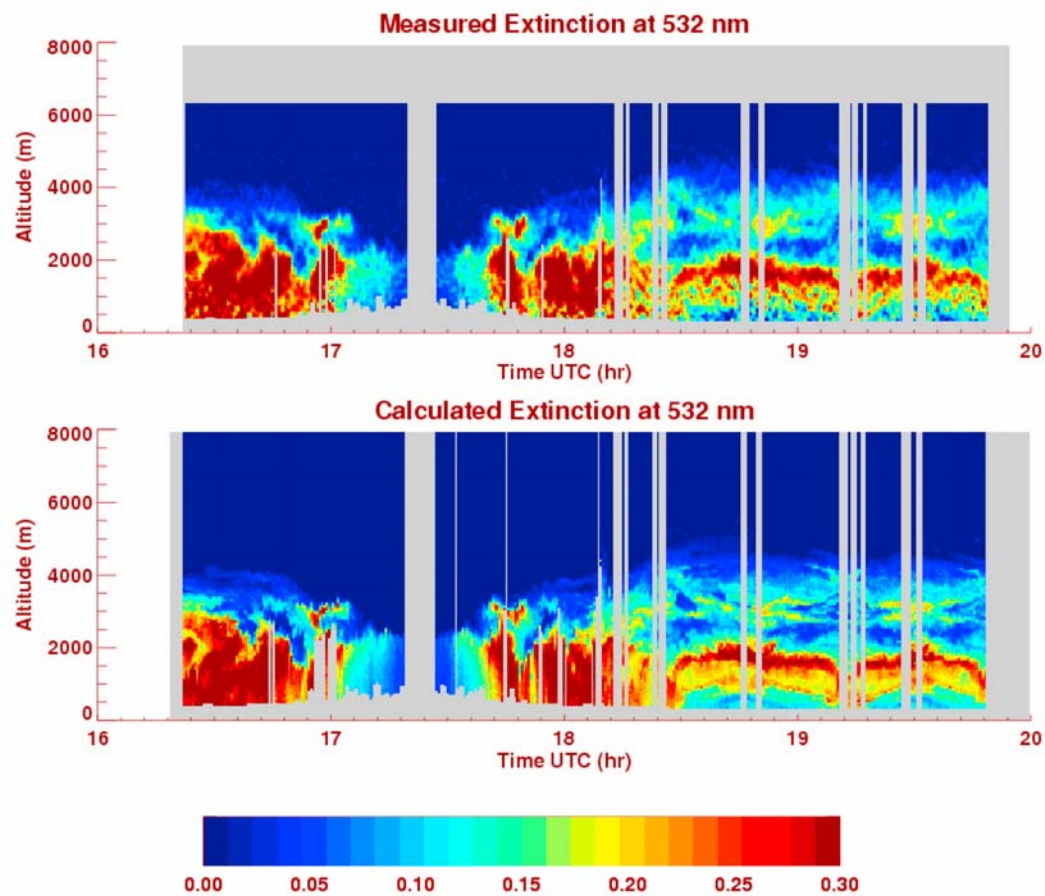

Figure 8. Aerosol extinction coefficient (km^{-1}) at 532 nm as derived from (top) the HSRL technique ("measured") and (bottom) the active-passive retrieval ("calculated") obtained from HSRL attenuated backscatter signal constrained by the HSRL AOT. These observations are from the flight on 4 August 2007 over the Mid-Atlantic states and off the coast of Virginia, as shown in Figure 2.

that is for larger values of AOT, aerosol extinction retrievals could be expected to improve with the use of the passive AOT constraint. The crossing point for the 30% uncertainty in CALIPSO S_a occurs at AOT values of approximately 0.15 for the MISR error bar and 0.2 for the MODIS land error bar. On the basis of Figure 1 and Figure 5, it seems that the reported uncertainty for MODIS AOT over water may be a slight underestimate, so we conservatively use the MISR threshold here as well. Accordingly, we set an AOT threshold of 0.2 for land and 0.15 for water and expect useful results from the active-passive retrieval for cases with AOT exceeding these thresholds.

5. Results of Active-Passive Retrieval With High Spectral Resolution Lidar (HSRL) Data

[22] For testing and initial validation of the algorithm, the constrained retrieval was first applied to HSRL attenuated backscatter data using the aerosol optical thickness derived from the HSRL technique. The HSRL attenuated backscatter data have the advantage of high resolution, high signal-to-noise ratio, and accurate calibration [*Hair et al.*, 2008]. By using the HSRL AOT as the constraint, perfect spatial and temporal coincidence is obtained between the backscatter profile and AOT measurements. This approach thus minimizes many factors that could complicate the assessment of the method.

[23] Figure 8 shows the results of the retrieval for the 3 hour HSRL flight on 4 August 2007 over the eastern United States and off the coast of Virginia. The results are shown as time-altitude cross sections of aerosol extinction coefficient beneath the aircraft. Figure 9 shows the median profile for the entire time period. Cloud attenuated lidar returns have been excluded from the retrieval. The agreement between the measured and retrieved aerosol extinction coefficient is very good. The percent difference is shown for each bin where the extinction coefficient is greater than 0.01 km^{-1}, which is each bin below 4.5 km. For these altitudes, the percent difference is between −4.8% and 11.3%. In this retrieval, the lidar ratio varies freely over time, but is assumed to be constant with altitude. These results indicate that the height variation is negligible for this case and the assumption of a constant lidar ratio with altitude is valid.

[24] The retrieval was performed for all HSRL flights between March 2006 and July 2008. This includes flights from the GoMACCS, MILAGRO, CHAPS, and ARCTAS campaigns (see Table 1 key) plus a field campaign in the San Joaquin valley in California in February 2007, a campaign in the Caribbean Sea in January and February 2008, and many underflights of CALIPSO in the Mid-

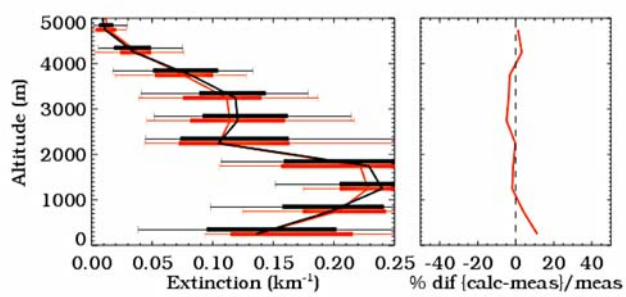

Figure 9. (left) Median profiles and (right) percentage difference profile in 0.5 km bins of the aerosol extinction coefficient retrieved from HSRL attenuated backscatter data constrained using the HSRL AOT (red lines), compared to the measured HSRL extinction (black lines), from the same flight as Figure 8. Cloudy shots have been excluded from the retrieval. The error bars show the 25th and 75th percentiles of the extinction values (bars) and the 5th and 95th percentiles (whiskers).

Atlantic states and off the coast of Virginia. Figure 10 shows a comparison of the aerosol extinction results for all cases combined. The linear bisector regression was made by considering each extinction coefficient at a given time and range from the instrument to be a separate comparison point. It should be emphasized, however, that the retrieved values of extinction coefficient at different ranges within the same profile are not independent. Retrieval profiles are included only if the HSRL AOT exceeds the thresholds derived above, 0.2 for land and 0.15 for water. The number of profiles included is 1258 from 63 different flights. The regression shows that the retrievals are unbiased. The linear correlation coefficients are 0.97 both over land and over water, confirming the excellent agreement between the retrieved and measured extinction coefficients. The root mean square (RMS) error is 0.02 km^{-1}. The data are heteroscedastic: the variability of the retrieved extinction is larger for larger extinction. For that reason, we also estimate an "error envelope" that varies with extinction, shown in this figure and following figures as broken lines. The envelope is defined such that at least two-thirds of the data agree within these bounds. Over water, the error envelope is ±0.0057 km^{-1} ± 10% of extinction. For land, the envelope is ±0.0065 km^{-1} ± 10%. These envelopes are determined manually and are necessarily somewhat subjective, since any number of combinations of an absolute and percent value can be formed to satisfy the criterion, but they are useful for quickly comparing one experiment to another. The figure itself is a more complete illustration of the comparison.

[25] The lidar ratios produced by the constrained retrieval are evaluated as a further test. As discussed above, one single range-independent value is obtained for each profile. The measurements obtained by the HSRL method are range-dependent, but a single equivalent lidar ratio for each profile is derived, for purposes of comparison, by computing the ratio of the sum of the measured aerosol extinction coefficient to the sum of the measured aerosol backscatter coefficient over all retrieved layers. The linear correlation between these lidar ratio estimates is 0.99 over water and 0.96 over land indicating excellent agreement. The agreement between the retrieval and the measurements for both aerosol extinction and lidar ratio indicate that the retrieval technique is sound.

[26] The retrieval must assume the lidar ratio is constant with altitude for each profile. The true variability of the lidar ratio can be estimated by examining the variability of measured lidar ratio values within each profile. The bulk of the 1258 profiles have a variability of 5–25 sr, as defined by the standard deviation of the measured lidar ratio values within each profile (see Figure 11). To gauge the effect of the assumption of constant lidar ratio, the comparison illustrated in Figure 10 is repeated for only those profiles that have a small variability in lidar ratio. The cutoff is 8 sr for the standard deviation of S_a, which limits the number of points in the regression to about 11–13% of the total. The regression is shown in Figure 12. No appreciable change is seen in the slope or correlation coefficient. The RMS error decreases from 0.024 km^{-1} to 0.013 km^{-1} for the water cases and from 0.023 km^{-1} to 0.015 km^{-1} for the land cases. The error envelopes which include two-thirds of the

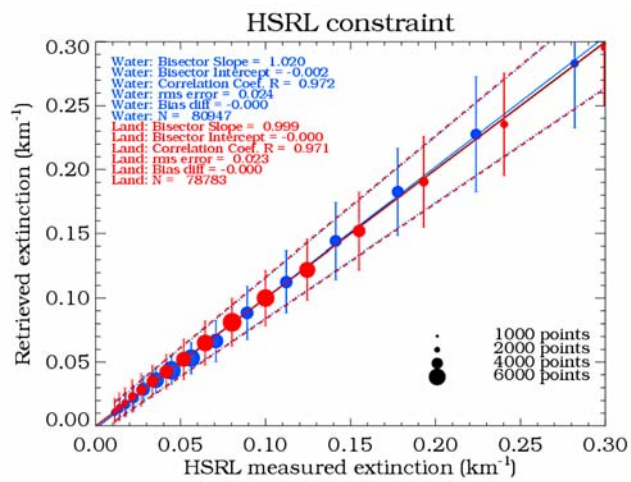

Figure 10. Comparison between measured aerosol extinction coefficient (HSRL technique) and the current retrieval, using the HSRL backscatter signal and HSRL AOT. The retrieval was done for all HSRL flights between March 2006 and February 2008, wherever column AOT exceeds 0.15 over water and 0.2 over land. A total of 1258 profiles during 63 flights are represented. Red shows results of retrievals over land, and blue shows retrievals over water. The red and blue lines represent the results of the linear bisector regression. For display purposes, points are sorted into bins in logarithmic space because of the relative abundance of cases with small extinction values (sorting and binning do not affect the linear regression). The circles show the mean value for each bin, while the error bars represent the standard deviation in each bin. The size of the circle is proportional to the number of points in the bin, as shown in the legend. The results of linear regressions are also shown in the legend. A black line denotes the one-to-one line. Error "envelopes" are given, which encompass approximately two-thirds of the data. The envelopes are ±0.0057 km^{-1} ± 10% (for ocean in blue) and ±0.0065 km^{-1} ± 10% (for land in red).

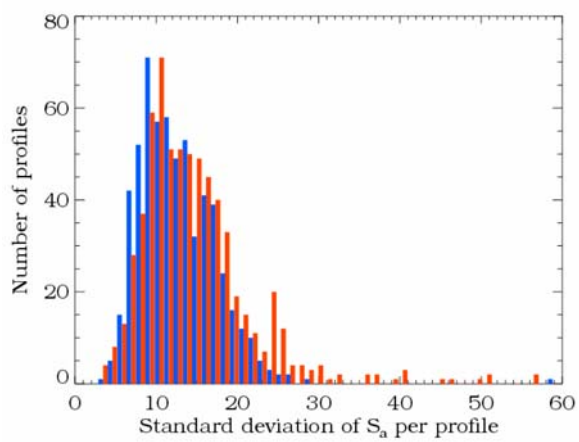

Figure 11. Vertical variability of the lidar ratio as measured by HSRL using the HSRL technique. For each vertical profile, the standard deviation of the lidar ratio is calculated, and these standard deviations are then shown as a histogram. Standard deviations for a given vertical profile range from ~5 sr to ~25 sr (with a small minority having much larger values). The profiles illustrated are the same as those used in Figure 10. Red and blue represent land and water measurements, as in other figures.

data are reduced to ±0.0061 km^{-1} ± 6% for both land and ocean. Therefore, it is likely that a significant amount of the deviation from the one-to-one line in Figure 10 is due to variability in the lidar ratio that is neglected in this retrieval. This is not unexpected. A measurement technique that directly measures lidar ratio, such as HSRL or Raman lidar, should produce more accurate extinction coefficient profiles without this additional error. Yet, this result demonstrates that a suitable column AOT constraint and the assumption of constant lidar ratio can enable reasonable retrievals of extinction coefficient profiles with uncertainties that may be acceptable for many applications.

6. Results of Active-Passive Retrieval Using HSRL Backscatter Signal With Satellite Aerosol Optical Thickness Constraint

[27] The constrained retrievals of extinction coefficients and lidar ratio using HSRL attenuated backscatter coefficients were repeated using coincident AOT measurements from the MODIS instrument on board Aqua. All HSRL measurements that occur within the boundaries of a given QA filtered MODIS pixel and within 3 h are considered to be coincident with that observation pixel. The retrieval is performed on HSRL attenuated backscatter profiles of 10 s (~1 km) horizontal resolution, and then the resulting extinction coefficients are averaged such that all profiles coincident with a given observation pixel are combined into a single profile, to preserve one-to-one correspondence with MODIS observations. The resolution of MODIS pixels is 10 × 10 km in the nadir direction, to about 40 × 10 km at the edge of a swath.

[28] The same 4 August 2007 flight, as shown above in Figure 8, is a useful example to illustrate the retrieval using MODIS Aqua aerosol optical thickness also. The results are displayed in Figure 13. Before 1825 UT, the Aqua-constrained retrievals exhibit very good agreement, but there is an obvious bias after that time. The biased retrieval is a direct consequence of a difference in the aerosol optical thickness between MODIS and HSRL after 1825 UT, when the aircraft flew out over water, as in Figure 2 and Figure 3. The segments of this flight over water belong to the set of very high AOT values that appear biased in the Aqua MODIS data in Figure 1.

[29] Aerosol extinction coefficients are derived for all possible cases using HSRL attenuated backscatter signal and Aqua MODIS AOT in Figure 14. The retrieval results shown here and those for Terra MODIS and MISR discussed later are only for cases where the column aerosol optical thickness as measured by the satellite exceeds 0.2 over land or 0.15 over water, as discussed above. The results of the retrieval using the Aqua constraint have a striking bias over water, with retrieved extinction coefficients progressively too small compared to the HSRL extinction coefficient as the extinction value increases. This bias is consistent with the bias seen in the AOT comparison shown in Figure 1. Otherwise, the bulk of the retrieved extinction values agree well with the HSRL measured values. The linear correlation coefficient for the regression between the HSRL measured extinction coefficient and retrieved extinction coefficient is 0.86 over water and 0.90 over land. The slope of the linear bisector regression over ocean is 0.73 reflecting the bias for large extinction, but for land the slope is 0.99. Error envelopes encompassing at least two-thirds of the data points are ±0.0061 km^{-1} ± 25% for Aqua MODIS over water and ±0.0090 km^{-1} ± 20% over land. Reducing the number of profiles by including only those with a small amount of variability in the HSRL measured lidar ratio, less than 8 sr, as discussed above for the HSRL case, reduces the RMS error in the regression from 0.046 km^{-1} only to 0.043 km^{-1} for cases over land (regression not illustrated). This is a much smaller reduction than was seen in the retrieval using the

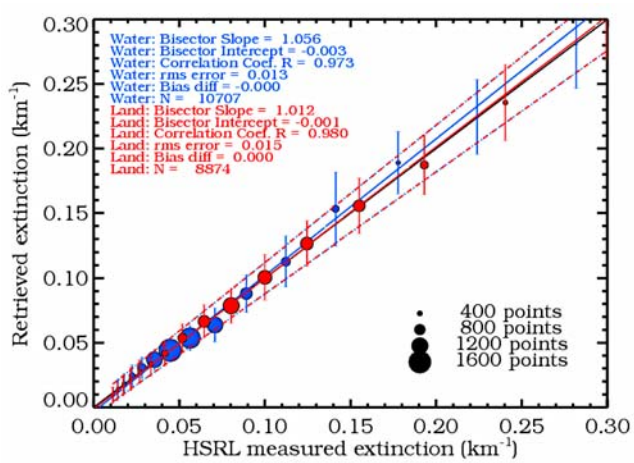

Figure 12. Comparison between the active-passive retrieval and the HSRL measurement, originally shown in Figure 10, repeated here only for profiles in which the standard deviation of the lidar ratio for each profile is 8 sr or less. Here the error envelopes, which contain at least two-thirds of the data, are ±0.0061 km^{-1} ± 6% for both land and ocean.

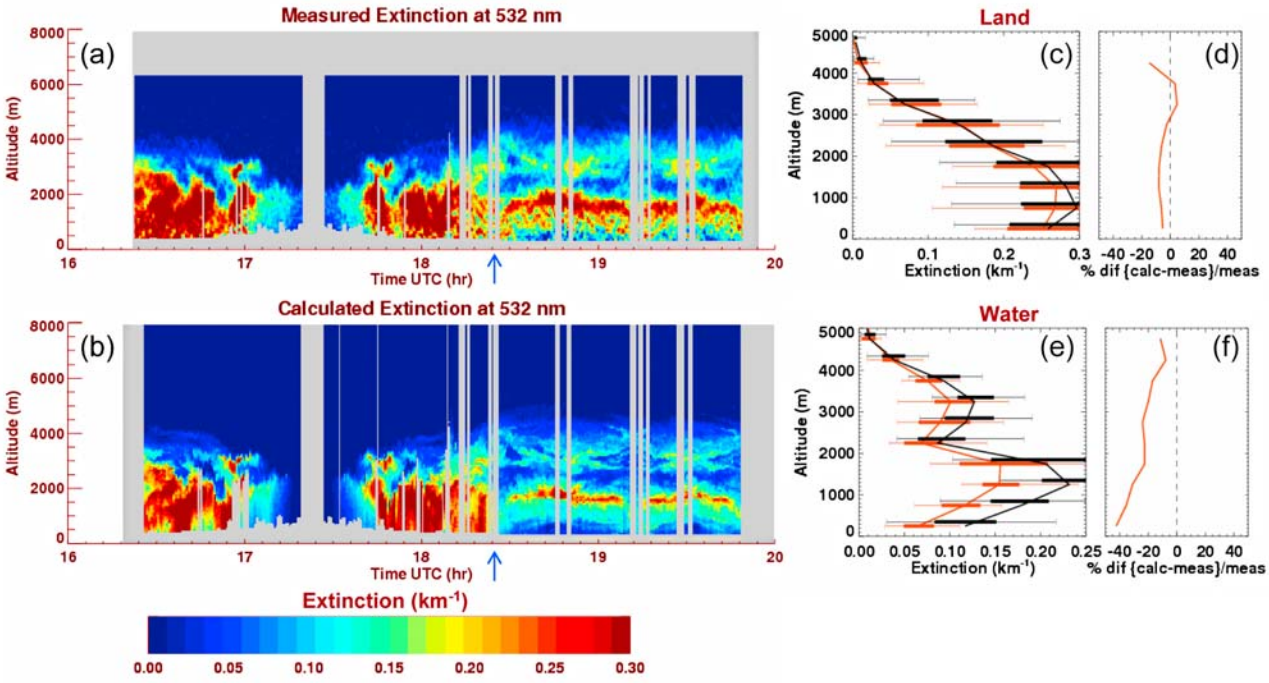

Figure 13. Aerosol extinction coefficient for the flight on 4 August 2007 off the coast of Virginia. The aircraft crossed the coast from land to water at approximately 1825 UT, marked with a blue arrow. (a) Measured extinction (using the HSRL technique) and (b) the results of the retrieval using MODIS Aqua AOT. For some shots where no retrieval is possible because there is no MODIS AOT information, aerosol extinction is derived using the S_a value linearly interpolated from nearby shots. These interpolated shots are included in cross-sectional figures like this one for readability, but are not included in statistical assessments of the retrieval, as shown in Figures 13c–13f and figures similar to Figure 14. Median profiles are shown for the (c) land and (e) ocean segments. The error bars show the 25th and 75th percentiles of the extinction values (bars) and the 5th and 95th percentiles (whiskers). Extinction from the retrieval is shown in red, and the measured HSRL extinction is shown in black. Percentage differences are shown for (d) the land portion and (f) the ocean portion in 0.5 km bins. Cloudy shots have been excluded from the retrieval.

HSRL AOT constraint. Other factors, specifically errors in aerosol optical thickness associated either with the AOT retrieval or with spatial and temporal variability, are more important contributors to the extinction retrieval errors in this case than the assumption of constant lidar ratio.

[30] The retrieved lidar ratio using the Aqua MODIS AOT constraint exhibits less correlation with the value derived from HSRL measurements (R = 0.77 over water and only 0.27 over land), as illustrated in Figure 15. The errors in lidar ratio are consistent with differences between HSRL and MODIS aerosol optical thickness shown above. There is a direct relationship between the error in lidar ratio and the difference between the MODIS AOT and HSRL measured AOT. Therefore, any future improvement to retrievals of aerosol optical thickness from satellites can potentially yield significant improvement of the retrieval of both lidar ratio and aerosol extinction coefficient; however, the extinction retrieval is less sensitive to small errors in AOT.

[31] Figure 16 shows the comparison of aerosol extinction coefficients from retrievals using AOT from MODIS on Terra, and Figure 17 shows the results using the MISR AOT. In contrast to Aqua MODIS, the extinction retrievals over water using AOT from MODIS on Terra and those using MISR AOT do not show such drastic bias. It would be fair to point out again however that the MISR retrievals do not include any cases with AOT greater than 0.6. Again, the bulk of the retrieved extinction values agree well with the HSRL measured values. The linear correlation coefficients for the regressions between the HSRL measured extinction coefficient and retrieved extinction coefficient for Terra MODIS and MISR, land and water, are between 0.85 and 0.90 for each case. For the Terra MODIS constraint, two-thirds of retrieval points fall within ±0.0082 km^{-1} ± 20% for ocean and ±0.0066 km^{-1} ± 20% for land. Using MISR, the envelopes encompassing two-thirds of retrieval points are ±0.0078 km^{-1} ± 20% over water and ±0.0064 km^{-1} ± 20% over land.

7. Results of Active-Passive Retrieval With CALIPSO Data

[32] Retrievals using the CALIPSO attenuated backscatter data were also performed. An example is shown in Figure 18, from a portion of the same 4 August 2007 flight. From about 1723 UT to 1813 UT, the B200 performed an underflight of the CALIPSO measurement track. For this retrieval, the CALIPSO attenuated backscatter data are

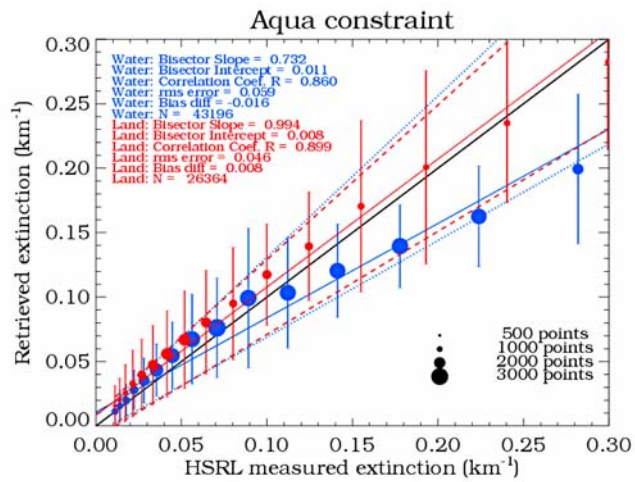

Figure 14. Same as Figure 10 but the active-passive extinction retrieval employs MODIS Aqua AOT data as the constraint rather than HSRL AOT. The retrieval is done for profiles in which there is valid Aqua MODIS AOT data within 3 hours of the HSRL observation. A total of 530 profiles are represented during 44 flights. After retrieval, HSRL profiles are combined to produce one profile per MODIS pixel. Aerosol extinction values for every 30 m in height from the combined profiles were used in the regressions and then binned according to the extinction coefficient to produce the figure. Manually determined error envelopes are shown, which contain two-thirds of the data. These are ±0.0061 km^{-1} ± 25% (water; blue) and ±0.009 km^{-1} ± 20% (land; red).

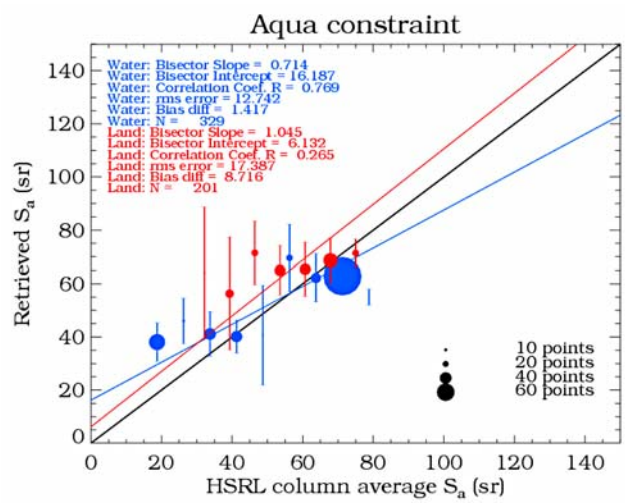

Figure 15. For the same set of retrievals as in Figure 14, the retrieved lidar ratio, S_a, depicted on the y axis compared to a measured value on the x axis. The actual measured lidar ratio is a function of range (or altitude), but for comparison, a single value for each profile was obtained by determining the ratio of the sum of the aerosol extinction coefficient in all retrieved layers to the sum of the aerosol backscatter coefficient in the same layers, where both the aerosol extinction and aerosol backscatter coefficients are the measured values obtained by the HSRL method. The lidar ratio depicted on the y axis is a product of the retrieval using the AOT from Aqua MODIS as a constraint.

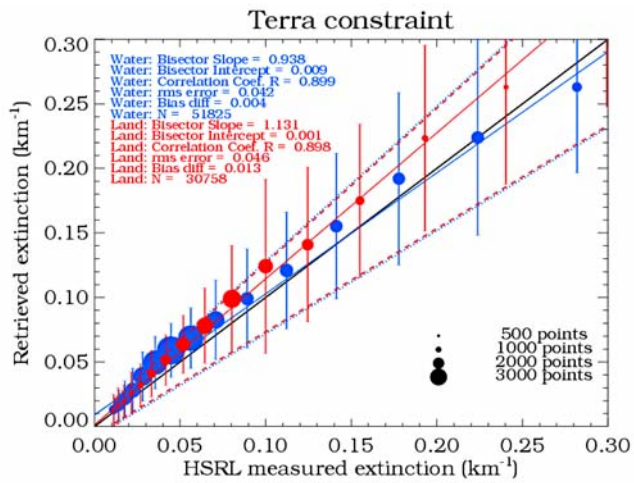

Figure 16. Same as Figure 14 but for MODIS on Terra. A total of 613 profiles are represented from 39 flights. Error envelopes are ±0.0082 km^{-1} ± 20% for ocean (blue) and ±0.0066 km^{-1} ± 20% for land (red).

averaged to a nominal 80 km horizontal resolution and the retrieval is performed as described above. The resulting extinction coefficient profile is then smoothed to 330 m vertical resolution, approximately equivalent to the vertical resolution of the HSRL measured aerosol extinction coefficient derived using the HSRL method. Figure 18 shows fairly good agreement between the CALIPSO-MODIS retrieval and the HSRL measurement for all four profiles, but the fourth profile exhibits some temporal mismatch. The B200 lagged behind the CALIPSO overpass by about 49 min by the time this fourth profile was observed. A small aerosol peak is visible at about 3000 m in the HSRL profile, but not the CALIPSO retrieval. In fact, the HSRL-MODIS retrieval, also shown in the figure, is obviously biased for this profile, most likely because the MODIS AOT

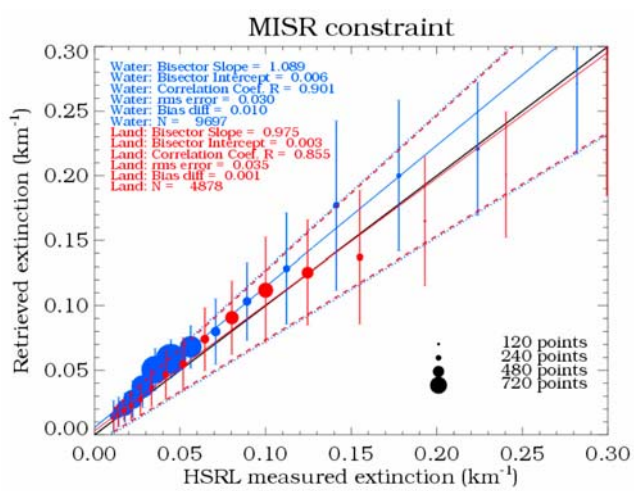

Figure 17. Same as Figure 14 but for the retrieval using HSRL attenuated backscatter signal and MISR AOT. A total of 114 profiles are represented from 13 flights. Error envelopes are ±0.0078 km^{-1} ± 20% for ocean (blue) and ±0.0064 km^{-1} ± 20% for land (red).

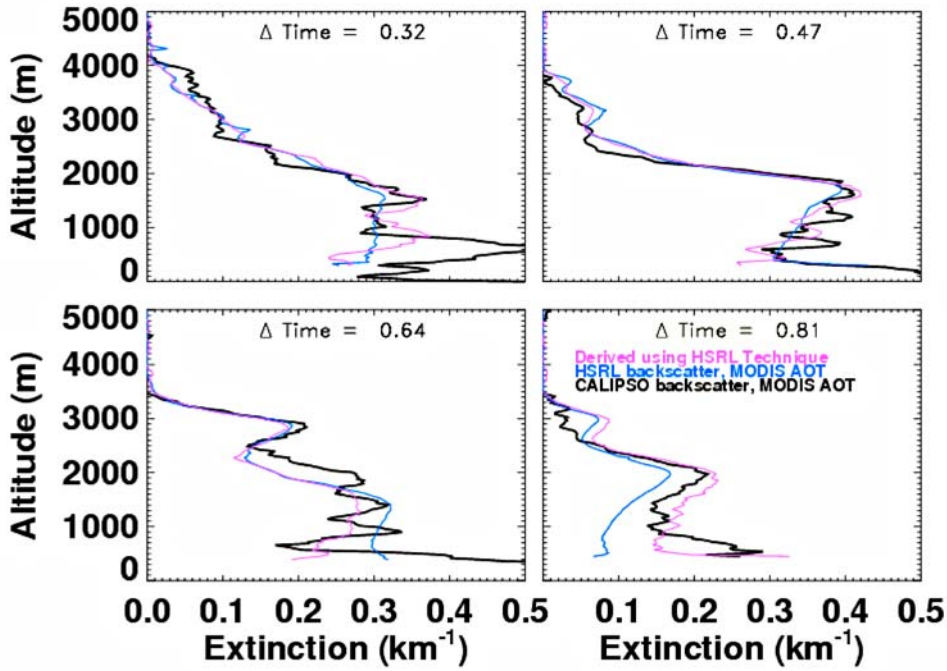

Figure 18. Aerosol extinction coefficient from an approximately 320 km flight segment on 4 August 2007, during which the HSRL instrument on board the NASA Langley B200 flew along the CALIPSO track. The HSRL flight time for this segment was approximately 38 min. The retrieval is performed on CALIPSO data averaged to 80 km segments with the MODIS Aqua aerosol thickness constraint. Results are shown in black. The HSRL measured aerosol extinction coefficient (magenta) and the retrieval performed on HSRL backscatter with the MODIS Aqua constraint (blue) are also shown, averaged to 80 km resolution, for comparison. The CALIPSO overpass was later than the B200 flight in this location; the average time difference between HSRL and CALIPSO (CALIPSO time minus HSRL time) is shown at the top of each panel in fractions of an hour.

observation, less than 1 min ahead of CALIPSO, does not include this secondary peak.

[33] The active-passive retrieval using CALIPSO backscatter signal and MODIS AOT was performed for 37 profiles (28 over land and 9 over water) on 18 flight dates between June 2006 and July 2008, in which there were HSRL measurements along the CALIPSO flight track, and for which MODIS AOT observations from Aqua pass the QA test and are greater than the thresholds of 0.15 over water and 0.2 over land discussed above. These profiles range over North America from 8.2°N to 61.3°N and from 60.0°W to 116.9°W.

[34] Figure 19 shows that the retrieved extinction coefficient agrees with the HSRL extinction coefficient for at least two-thirds of cases with extinction exceeding 0.02 km^{-1} within ±0.016 km^{-1} ± 20% over land and within ±0.028 km^{-1} ± 20% over water. The lower limit of 0.02 km^{-1} was incorporated only for the sake of defining an error envelope that adequately reflects the quality of the results for nontrivial extinction values. If all points are used, including those in clear air in the 2000 m above the highest feature in the vertical feature mask, agreement within these bounds occurs for 67% of land points and 87% of ocean points.

[35] In general, the CALIPSO active-passive retrieval produces very good agreement with the coincident HSRL measurements. The success of the retrieval is logically limited by the accuracy and precision of the Aqua MODIS AOT that is used to constrain it, and to a lesser extent, by the vertical variability in the lidar ratio. The results demonstrate that the constant lidar ratio assumption, along with a suitable column AOT constraint, produces extinction profiles whose uncertainties compare favorably with the original CALIPSO measurement requirement of 40% uncertainty [*Winker et al.*, 2009]. Nevertheless, as discussed in section 5, a measurement technique that is able to capture the variability of the lidar ratio, such as HSRL or Raman lidar, will produce still more accurate extinction coefficient profiles in the large number of cases where significant variability of the lidar ratio translates to additional uncertainty in the retrieval.

[36] In the current study, some retrievals do not produce good agreement simply because the AOT constraint is poor for some cases, as shown in Figure 1. The retrievals discussed here also include some cases in which the disagreement reflects atmospheric variability between the times of HSRL and CALIPSO measurements, as in the fourth profile on 4 August 2007. As discussed above, for the bulk of comparisons, a 3 hour coincidence window is believed to be adequate, but it is likely that individual cases remain, like this one, with an exceptional degree of variability. Narrowing the coincidence criterion to 30 min does not significantly improve the statistics of the comparisons. Over land, the linear correlation coefficient increases from 0.86 to 0.93

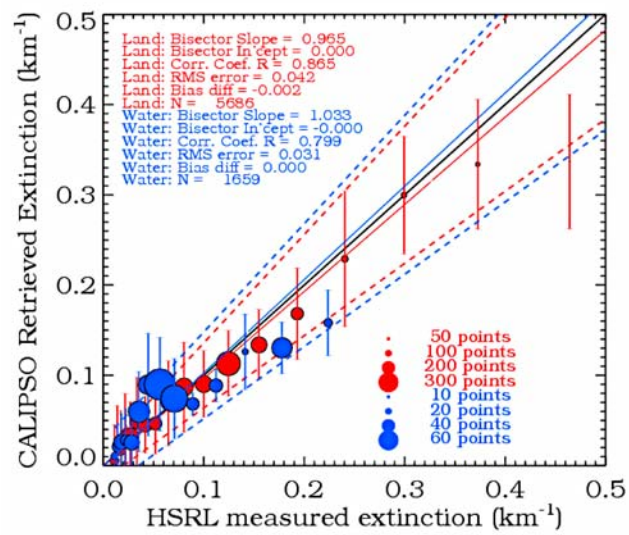

Figure 19. Comparison of aerosol extinction coefficient with HSRL for all the CALIPSO + MODIS retrievals. The retrieval was done for all HSRL coincidences in which the AOT exceeds 0.2 over land or 0.15 over water. It is performed at 80 km horizontal resolution, and the CALIPSO profiles are smoothed to 330 m vertical resolution after the retrieval to approximate the HSRL resolution. Nine profiles over water and 28 profiles over land are shown. Error envelopes are ±0.028 km^{-1} ± 20% for ocean (blue) and ±0.016 km^{-1} ± 20% for land (red). These encompass two-thirds of retrieved points with measured extinction values greater than 0.02 km^{-1}. If smaller extinctions are included, the percentages are 87% (ocean) and 67% (land). For better readability in the graph, the points were binned, and the averages and standard deviations of each bin are shown. Because of the much greater fraction of points over land, the scales are not equal between water and land, but both scales are illustrated.

and the RMS error decreases somewhat from 0.042 km^{-1} to 0.029 km^{-1}, while the slope and bias difference change only slightly (slope changes from 0.96 to 1.02 and bias difference changes from −0.002 km^{-1} to 0.001 km^{-1}). Over water, limiting to 30 min coincidence has an even smaller effect, increasing R from 0.80 to 0.86, changing the slope from 1.03 to 0.96, but not changing the RMS (still 0.031 km^{-1}) and making the bias difference slightly worse from 0.000 km^{-1} to −0.005 km^{-1}. In short, it is probable that in cases with large atmospheric variability, imperfect coincidence may lead to some inaccuracy in the retrieval; however, the bulk of retrievals with time differences up to 3 hours are successful.

[37] A final example is shown in Figure 20. In this case, the provisional 2.01 CALIPSO product is shown and the comparison illustrates a primary benefit of the active-passive retrieval technique described here. This profile was observed on 28 August 2006 near Houston, during the Texas Air Quality Study and Gulf of Mexico Atmospheric Composition and Climate Study (TexAQS/GoMACCS 2006). During this study aerosol measured in the Gulf of Mexico during onshore flow was highly impacted by Saharan dust [*Bates et al.*, 2008]. The dust observed on 28 August 2006 originated as a dust storm on 17 August and was tracked across the Atlantic by CALIPSO observations starting on 18 August [*Liu et al.*, 2008]. This CALIOP aerosol extinction profile has been individually selected from the generally unvalidated beta product and was cleared for use by the CALIOP processing team. The CALIOP feature finder identifies a layer of dust between 1.5 and 3 km and both dust and polluted dust at lower altitudes. Inspection of the data for this individual profile, particularly the depolarization data, from both CALIOP and HSRL, confirms that the identification of dust in this particular profile is correct. However, the lidar ratios provided by the CALIOP aerosol models for this case are much higher, 40 sr for dust and 65 sr for polluted dust [*Omar et al.*, 2009], than what is obtained by the active-passive retrieval or measured by the HSRL instrument using the HSRL technique, particularly below 1.5 km. The lidar ratio from the measurement ranged from 28.7 to 38.5 below 1.5 km and up to 49.9 sr between 1.5 and 3 km. The active-passive retrieval obtained a value of about 42 sr for the profile as a whole, which is approximately the average of the measured lidar ratios, as expected. In a case like this, although the CALIOP layer detection and typing algorithm is performing exactly as designed, the need for a priori assumptions about the optical properties of the aerosol types shows as a limitation, since the optical properties of a given aerosol type can vary considerably. The active-passive retrieval, which does not require an assumption of the lidar ratio, provides an indication that a

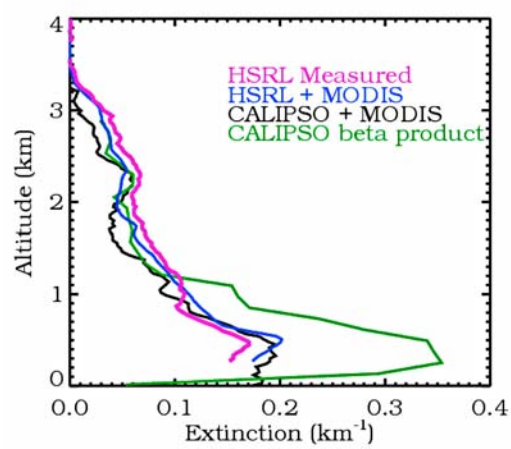

Figure 20. Saharan dust observation made by HSRL and CALIPSO on 28 August 2006 near Houston. The aerosol extinction coefficients at 532 nm are shown from the active-passive retrieval using a CALIPSO attenuated backscatter signal (black) and a HSRL attenuated backscatter signal (blue), both constrained by MODIS Aqua AOT. In magenta is shown the HSRL aerosol extinction measurement. The provisional Cloud-Aerosol Lidar with Orthogonal Polarization (CALIOP) version 2.01 aerosol extinction profile is shown in green. In this case, the CALIOP and HSRL attenuated backscatter observations are in agreement, but the lidar ratio assigned by the CALIOP retrieval is significantly larger than what is measured by HSRL or obtained by the active-passive retrieval, leading to a large discrepancy in the aerosol extinction coefficient.

smaller lidar ratio is required here. As mentioned earlier, errors in the operational retrieval due to incorrect lidar ratios are of particular concern for near-surface applications, since such errors propagate downward [*Young and Vaughan*, 2009]. Therefore, the active-passive technique might be expected to improve the suitability of CALIPSO observations for air-quality studies, particularly in high loading cases as we have studied here, in which the $PM_{2.5}$ levels are most likely to be in noncompliance with Environmental Protection Agency standards. When the CALIPSO product has been released, a more comprehensive comparison of the active-passive retrieval with the CALIPSO product will be undertaken.

8. Summary

[38] The NASA Langley airborne HSRL measurements have provided the opportunity to test and validate an active-passive retrieval of aerosol extinction profiles at 532 nm from CALIPSO attenuated lidar backscatter data. This retrieval of aerosol extinction at 532 nm via Fernald inversion uses coincident passive satellite aerosol optical thickness observations as a constraint. The retrieval can be performed over land and water, anywhere a coincident aerosol optical thickness measurement at 532 nm can be obtained. A primary advantage of this technique is that no knowledge of aerosol type or lidar ratio is required. Coincidences between CALIPSO, HSRL and MODIS on Aqua have allowed the retrieval to be performed and evaluated for 37 profiles with 80 km horizontal resolution. To ameliorate the effect of large uncertainty for small aerosol optical thickness measurements, and to maximize the impact of the active-passive retrieval in comparison with the current CALIPSO retrieval that is more effective for small AOT, the retrievals were limited to cases with MODIS AOT greater than 0.2 over land or 0.15 over water. The resulting extinction coefficient compares well with extinction measured coincidentally with the HSRL instrument using the HSRL technique, specifically within ± 0.016 km^{-1} $\pm$ 20% for retrieved extinction coefficients over land and within ± 0.028 km^{-1} $\pm$ 20% over water, for two-thirds of extinction coefficients exceeding 0.02 km^{-1}. Additional analysis of this retrieval, in comparison to CALIPSO operational products, will proceed after the CALIPSO product release.

[39] The most important sources of systematic error are errors in the satellite aerosol optical thickness used to constrain the retrieval. These errors can arise either from systematic errors in the AOT observations themselves, or from spatiotemporal mismatch between the lidar and the AOT footprints. Another smaller source of error is the assumption of constant lidar ratio that is required for this retrieval.

[40] More precise aerosol optical thickness measurements, such as those expected from the Aerosol Polarimetry Sensor (APS), would directly lead to improvements of this active-passive retrieval from CALIPSO measurements. APS is part of the NASA Glory mission [*Mishchenko et al.*, 2007], which is to join the "A-train" satellite constellation in 2010. A precursor instrument, the Research Scanning Polarimeter (RSP) [*Waquet et al.*, 2009] has flown with HSRL aboard the NASA B-200 aircraft since June 2008; the combination provides a means of testing a similar combination of measurements.

[41] A limitation of this retrieval is that it requires a coincident measurement of aerosol optical thickness. Combined CALIPSO-MODIS aerosol retrievals therefore can only be obtained with this technique during daytime, and it is not appropriate in sun glint regions or over bright snow where MODIS measurements are not available. Other combined aerosol retrieval techniques with different strengths and limitations are currently being investigated by other researchers. It is likely that no single technique will prove best under all circumstances, and some strategy of combining multiple methods will provide the most robust aerosol retrievals for CALIPSO. For example, the CRAM technique [*McPherson et al.*, 2010] which constrains retrievals using aerosol models derived from AERONET measurements rather than coincident measurements from a passive satellite sensor may be of particular interest for nighttime CALIPSO observations.

[42] To improve this active-passive retrieval any further, or indeed any active-passive retrieval relying on MODIS aerosol optical thickness measurements, it would be desirable to gain a better understanding of the apparent bias of aerosol optical thickness as observed by MODIS on board Aqua for large values of AOT over ocean in August 2007. There is no similar disagreement evident between HSRL and Terra MODIS AOT, leading us to provisionally characterize the bias as belonging to Aqua MODIS rather than HSRL. Unfortunately, the small number of flights during which such large AOT was observed makes it difficult to characterize. Further investigation into the apparent bias is called for.

[43] Finally, it should be noted that the HSRL technique, which provided the "truth" measurements of aerosol extinction used in this study, is currently being pursued for space-based operations. This technique does not require additional coincident measurements of optical thickness and should provide more accurate aerosol extinction profiles by measuring the vertical variability of the lidar ratio.

[44] **Acknowledgments.** The CALIPSO and MISR data used here were obtained from the NASA Langley Research Center Atmospheric Science Data Center. We also acknowledge the ICARE Data and Service Center for providing access to the PARASOL data used in this study. Funding for this research came from the NASA HQ Science Mission Directorate Radiation Sciences Program, the NASA CALIPSO and MODIS projects, and the Department of Energy Atmospheric Science Program (Interagency Agreement DE-AI02-05ER6398). The authors would also like to thank the NASA Langley B200 King Air flight crew for their outstanding work in supporting the HSRL measurements.

References

Anselmo, T., et al. (2007), Cloud–aerosol LIDAR infrared Pathfinder satellite Observations Data Management System data products catalog, release 2.4, *Doc. PC-SCI-503*, NASA Langley Research Center, Hampton, Va.

Bates, T. S., et al. (2008), Boundary layer aerosol chemistry during TexAQS/GoMACCS 2006: Insights into aerosol sources and transformation processes, *J. Geophys. Res.*, *113*, D00F01, doi:10.1029/2008JD010023.

Bosenberg, J., et al. (2001), EARLINET: A European Aerosol Research Lidar Network, in *Laser Remote Sensing of the Atmosphere: Selected Papers of the 20th International Laser Radar Conference, Vichy, France*, edited by A. Dabas, C. Loth, and J. Pelon, pp. 155–158, École Polytech., Paris.

Davis, K. J., N. Gamage, C. R. Hagelberg, C. Kiemle, D. H. Lenschow, and P. P. Sullivan (2000), An objective method for deriving atmospheric

structure from airborne lidar observations, *J. Atmos. Oceanic Technol.*, *17*, 1455–1468, doi:10.1175/1520-0426(2000)017<1455:AOMFDA>2.0.CO;2.

Fernald, F. G. (1984), Analysis of atmospheric lidar observations: Some comments, *Appl. Opt.*, *23*, 652–653, doi:10.1364/AO.23.000652.

Fernald, F. G., B. M. Herman, and J. A. Reagan (1972), Determination of aerosol height distributions by lidar, *J. Appl. Meteorol.*, *11*, 482–489, doi:10.1175/1520-0450(1972)011<0482:DOAHDB>2.0.CO;2.

Ferrare, R. A., D. D. Turner, L. Heilman Brasseur, W. F. Feltz, O. Dubovik, and T. P. Tooman (2001), Raman lidar measurements of the aerosol extinction-to-backscatter ratio over the Southern Great Plains, *J. Geophys. Res.*, *106*, 20,333–20,347.

Ferrare, R. A., et al. (2006), The vertical distribution of aerosols: Lidar measurements vs. model simulations, paper presented at the 23rd International Laser Radar Conference, INDECO, Inc., Nara, Japan, 24–28 July.

Grund, C. J., and E. W. Eloranta (1991), The Univ. of Wisconsin high spectral resolution lidar, *Opt. Eng.*, *30*, 6–12, doi:10.1117/12.55766.

Hair, J. W., C. A. Hostetler, A. L. Cook, D. B. Harper, R. A. Ferrare, T. L. Mack, W. Welch, L. R. Izquierdo, and F. E. Hovis (2008), Airborne high spectral resolution lidar for profiling aerosol optical properties, *Appl. Opt.*, *47*, 6734–6752, doi:10.1364/AO.47.006734.

Hansen, J., et al. (2007), Climate simulations for 1880–2003 with GISS modelE, *Clim. Dyn.*, *29*, 661–696, doi:10.1007/s00382-007-0255-8.

Haywood, J. M., et al. (1997), A limited-area-model case study of the effects of sub-grid scale variations in relative humidity and cloud upon the direct radiative forcing of sulfate aerosol, *Geophys. Res. Lett.*, *24*, 143–146, doi:10.1029/96GL03812.

Holben, B. N., et al. (1998), AERONET—A federated instrument network and data archive for aerosol characterization, *Remote Sens. Environ.*, *66*, 1–16, doi:10.1016/S0034-4257(98)00031-5.

Hunt, W. H., D. M. Winker, M. A. Vaughan, K. A. Powell, P. L. Lucker, and C. Weimer (2009), CALIPSO lidar description and performance assessment, *J. Atmos. Oceanic Technol.*, *26*, 1214–1228, doi:10.1175/2009JTECHA1223.1.

Isobe, T., E. D. Feigelson, M. G. Akritas, and G. J. Babu (1990), Linear regression in astronomy I, *Astrophys. J.*, *364*, 104–113, doi:10.1086/169390.

Jäger, H. (2005), Long-term record of lidar observations of the stratospheric aerosol layer at Garmisch-Partenkirchen, *J. Geophys. Res.*, *110*, D08106, doi:10.1029/2004JD005506.

Kahn, R. A., B. J. Gaitley, J. V. Martonchick, D. J. Diner, and K. A. Crean (2005), Multiangle Imaging Spectroradiometer (MISR) global aerosol optical depth validation based on 2 years of coincident Aerosol Robotic Network (AERONET) observations, *J. Geophys. Res.*, *110*, D10S04, doi:10.1029/2004JD004706.

Kaufman, Y. J., J. M. Haywood, P. V. Hobbs, W. Hart, R. Kleidman, and B. Schmid (2003), Remote sensing of vertical distributions of smoke aerosol off the coast of Africa during SAFARI 2000, *Geophys. Res. Lett.*, *30*(16), 1831, doi:10.1029/2003GL017068.

Klett, J. D. (1981), Stable analytical inversion solution for processing lidar returns, *Appl. Opt.*, *20*, 211–220, doi:10.1364/AO.20.000211.

Leon, J.-F., et al. (2003), Profiling of a Saharan dust outbreak based on a synergy between active and passive remote sensing, *J. Geophys. Res.*, *108*(D18), 8575, doi:10.1029/2002JD002774.

Liu, Z., et al. (2008), CALIPSO lidar observations of the optical properties of Saharan dust: A case study of long-range transport, *J. Geophys. Res.*, *113*, D07207, doi:10.1029/2007JD008878.

Liu, Z., M. Vaughan, D. Winker, C. Kittaka, B. Getzewich, R. Kuehn, A. Omar, K. Powell, C. Trepte, and C. Hostetler (2009), The CALIPSO lidar cloud and aerosol discrimination: Version 2 algorithm and initial assessment of performance, *J. Atmos. Oceanic Technol.*, *26*, 1198–1213, doi:10.1175/2009JTECHA1229.1.

McGill, M. J., D. L. Hlavka, W. D. Hart, E. J. Welton, and J. R. Campbell (2003), Airborne lidar measurements of aerosol optical properties during SAFARI-2000, *J. Geophys. Res.*, *108*(D13), 8493, doi:10.1029/2002JD002370.

McPherson, C. J., J. A. Reagan, J. Schafer, D. Giles, R. A. Ferrare, J. W. Hair, and C. A. Hostetler (2010), AERONET, airborne HSRL and CALIPSO aerosol retrievals compared and combined: A case study, *J. Geophys. Res.*, doi:10.1029/2009JD012389, in press.

Mishchenko, M. I., B. Cairns, G. Kopp, C. F. Schueler, B. A. Fafaul, J. E. Hansen, R. J. Hooker, T. Itchkawich, H. B. Maring, and L. D. Travis (2007), Accurate monitoring of terrestrial aerosols and total solar irradiance: Introducing the Glory mission, *Bull. Am. Meteorol. Soc.*, *88*, 677–691, doi:10.1175/BAMS-88-5-677.

Muller, D. E. (1956), A method for solving algebraic equations using an automatic computer, *Math. Tables Aids Comput.*, *10*, 208–215.

Omar, A. H., et al. (2009), The CALIPSO automated aerosol classification and lidar ratio selection algorithm, *J. Atmos. Oceanic Technol.*, *26*, 1994–2014, doi:10.1175/2009JTECHA1231.1.

Powell, K. A., et al. (2009), CALIPSO lidar calibration algorithms. Part I: Nighttime 532-nm parallel channel and 532-nm perpendicular channel, *J. Atmos. Oceanic Technol.*, *26*, 2015–2033, doi:10.1175/2009JTECHA1242.1.

Press, W. H., S. A. Teukolsky, W. T. Vetterling, and B. P. Flannery (1992), *Numerical Recipes in FORTRAN: The Art of Scientific Computing*, 2nd ed., Cambridge Univ. Press, New York.

Remer, L. A., et al. (2005), The MODIS aerosol algorithm, products, and validation, *J. Atmos. Sci.*, *62*, 947–973, doi:10.1175/JAS3385.1.

Remer, L. A., et al. (2008), Global aerosol climatology from the MODIS satellite sensors, *J. Geophys. Res.*, *113*, D14S07, doi:10.1029/2007JD009661.

Rogers, R. R., et al. (2009), NASA LaRC airborne high spectral resolution lidar aerosol measurements during MILAGRO: Observations and validation, *Atmos. Chem. Phys.*, *9*, 4811–4826.

Sasano, Y., E. V. Browell, and S. Ismail (1985), Error caused by using a constant extinction/backscattering ratio in the lidar solution, *Appl. Opt.*, *24*, 3929–3932, doi:10.1364/AO.24.003929.

Schmid, B., et al. (2006), How well do state-of-the-art techniques measuring the vertical profile of tropospheric aerosol extinction compare?, *J. Geophys. Res.*, *111*, D05S07, doi:10.1029/2005JD005837.

She, C.-Y. (2001), Spectral structure of laser light scattering revisited: Bandwidths of nonresonant scattering lidars, *Appl. Opt.*, *40*, 4875–4884, doi:10.1364/AO.40.004875.

Stephens, G. L., R. J. Engelen, M. Vaughan, and T. L. Anderson (2001), Toward retrieving properties of the tenuous atmosphere using space-based measurements, *J. Geophys. Res.*, *106*(D22), 28,143–28,157.

Thomason, L., and T. Peter (Eds.) (2006), Assessment of stratospheric aerosol properties (ASAP), *SPARC Rep. 4, WMO/TD 1295, Tech Rep. WCRP-124*, World Clim. Res. Prog., Geneva, Switzerland.

Thomason, L. W., S. P. Burton, B.-P. Luo, and T. Peter (2008), SAGE II measurements of stratospheric aerosol properties at non-volcanic levels, *Atmos. Chem. Phys.*, *8*, 983–995.

Vaughan, M., S. Young, D. Winker, K. Powell, A. Omar, Z. Liu, Y. Hu, and C. Hostetler (2004), Fully automated analysis of space-based lidar data: An overview of the CALIPSO retrieval algorithms and data products, *Proc. SPIE*, *5575*, 16–30.

Vaughan, M. A., K. A. Powell, R. E. Kuehn, S. A. Young, D. M. Winker, C. A. Hostetler, W. H. Hunt, Z. Liu, M. J. McGill, and B. J. Getzewich (2009), Fully automated detection of cloud and aerosol layers in the CALIPSO lidar measurements, *J. Atmos. Oceanic Technol.*, *26*, 2034–2050, doi:10.1175/2009JTECHA1228.1.

Waquet, F., B. Cairns, K. Knobelspiesse, J. Chowdhary, L. D. Travis, B. Schmid, and M. I. Michchenko (2009), Polarimetric remote sensing of aerosols over land, *J. Geophys. Res.*, *114*, D01206, doi:10.1029/2008JD010619.

Winker, D. M., W. H. Hunt, and M. J. McGill (2007), Initial performance assessment of CALIOP, *Geophys. Res. Lett.*, *34*, L19803, doi:10.1029/2007GL030135.

Winker, D. M., M. A. Vaughan, A. Omar, Y. Hu, K. A. Powell, Z. Liu, W. H. Hunt, and S. A. Young (2009), Overview of the CALIPSO mission and CALIOP data processing algorithms, *J. Atmos. Oceanic Technol.*, *26*, 2310–2323, doi:10.1175/2009JTECHA1281.1.

Young, S. A. (1995), Analysis of lidar backscatter profiles in optically thin clouds, *Appl. Opt.*, *34*, 7019–7031, doi:10.1364/AO.34.007019.

Young, S. A., and M. A. Vaughan (2009), The retrieval of profiles of particulate extinction from Cloud-Aerosol Lidar Infrared Pathfinder Satellite Observations (CALIPSO) data: Algorithm description, *J. Atmos. Oceanic Technol.*, *26*, 1105–1119, doi:10.1175/2008JTECHA1221.1.

S. P. Burton, Science Systems and Applications Inc., 1 Enterprise Pkwy., Ste. 200, Hampton, VA 23669, USA. (sharon.p.burton@nasa.gov)

A. L. Cook, R. A. Ferrare, J. W. Hair, D. B. Harper, C. A. Hostetler, M. D. Obland, R. R. Rogers, and M. A. Vaughan, NASA Langley Research Center, MS 401A, Hampton, VA 23681, USA.

L. A. Remer, NASA Goddard Space Flight Center, Greenbelt, MD 20771, USA.